Title

Tetrahymena Poc1 ensures proper intertriplet microtubule linkages to maintain basal body integrity

Journal

Molecular Biology of the Cell, 27(15)

ISSN

1059-1524

Authors

Meehl, Janet B
Bayless, Brian A
Giddings, Thomas H
et al.

Publication Date

2016-08-01

DOI

10.1091/mbc.e16-03-0165

Peer reviewed

Tetrahymena Poc1 ensures proper intertriplet microtubule linkages to maintain basal body integrity

Janet B. Meehl[a], Brian A. Bayless[b], Thomas H. Giddings, Jr.[a], Chad G. Pearson[b,†,*], and Mark Winey[a,†,*]

[a]Molecular, Cellular and Developmental Biology, University of Colorado at Boulder, Boulder, CO 80309; [b]Department of Cell and Developmental Biology, University of Colorado–Anschutz Medical Campus, Aurora, CO 80045

ABSTRACT **Basal bodies comprise nine symmetric triplet microtubules that anchor forces produced by the asymmetric beat pattern of motile cilia. The ciliopathy protein Poc1 stabilizes basal bodies through an unknown mechanism. In poc1Δ cells, electron tomography reveals subtle defects in the organization of intertriplet linkers (A-C linkers) that connect adjacent triplet microtubules. Complete triplet microtubules are lost preferentially near the posterior face of the basal body. Basal bodies that are missing triplets likely remain competent to assemble new basal bodies with nine triplet microtubules, suggesting that the mother basal body microtubule structure does not template the daughter. Our data indicate that Poc1 stabilizes basal body triplet microtubules through linkers between neighboring triplets. Without this stabilization, specific triplet microtubules within the basal body are more susceptible to loss, probably due to force distribution within the basal body during ciliary beating. This work provides insights into how the ciliopathy protein Poc1 maintains basal body integrity.**

Monitoring Editor
Stephen Doxsey
University of Massachusetts

Received: Mar 14, 2016
Revised: May 17, 2016
Accepted: May 27, 2016

INTRODUCTION

Centrioles are microtubule-organizing centers that play fundamental roles in building both centrosomes and cilia. Centriole defects disrupt normal centrosome and ciliary functions, contributing to an array of devastating human diseases ranging from cilia-related disorders, known collectively as ciliopathies, to cancer (Fliegauf *et al.*, 2007; Nigg and Raff, 2009; Waters and Beales, 2011; Gönczy, 2015). In the case of centrosomes, centrioles organize the pericentriolar material, which is the major site of microtubule organization in the cell. Such organization is important for spindle formation and function. In addition, centrioles also function as basal bodies to organize both primary and motile cilia. Primary cilia play critical roles in cell signaling, and motile cilia are responsible for cell motility and directed fluid flow. A unifying feature of centrioles and basal bodies as microtubule-organizing centers is the ability to withstand mechanical forces. Centrosomes experience mechanical forces from the mitotic spindle to ensure proper chromosome segregation (Abal *et al.*, 2005). Basal bodies, especially at motile cilia, experience mechanical forces from ciliary movement and beating (Lindemann and Kanous, 1997; Vernon and Woolley, 2004; Riedel-Kruse *et al.*, 2007; Bayless *et al.*, 2012; Galati *et al.*, 2014). However, the mechanisms by which centrioles and basal bodies resist mechanical forces remain poorly defined.

Despite their distinct functions in centrosomal and ciliary organization, centrioles and basal bodies have a conserved structure consisting of nine triplet microtubules that are symmetrically organized in a cylinder ~200 nm in diameter and 500 nm in length. Each triplet microtubule blade is composed of a 13 protofilament A-tubule, with 10 protofilament B- and C-tubules sequentially fused to the side of the A-tubule. In most basal bodies, C-tubules terminate at the transition zone, and the A- and B-tubules continue as doublet microtubules into the ciliary axoneme. Intertriplet linkers connect the triplet microtubule blades and are referred to as A-C linkers because these structures connect the A-tubule of one triplet microtubule to the C-tubule of an adjacent triplet microtubule (Gibbons and Grimstone, 1960; Li *et al.*, 2012; Guichard *et al.*, 2013).

This article was published online ahead of print in MBoC in Press (http://www.molbiolcell.org/cgi/doi/10.1091/mbc.E16-03-0165) on June 1, 2016.

†These authors contributed equally.

*Address correspondence to: Chad G. Pearson (Chad.Pearson@ucdenver.edu), Mark Winey (Mark.Winey@colorado.edu).

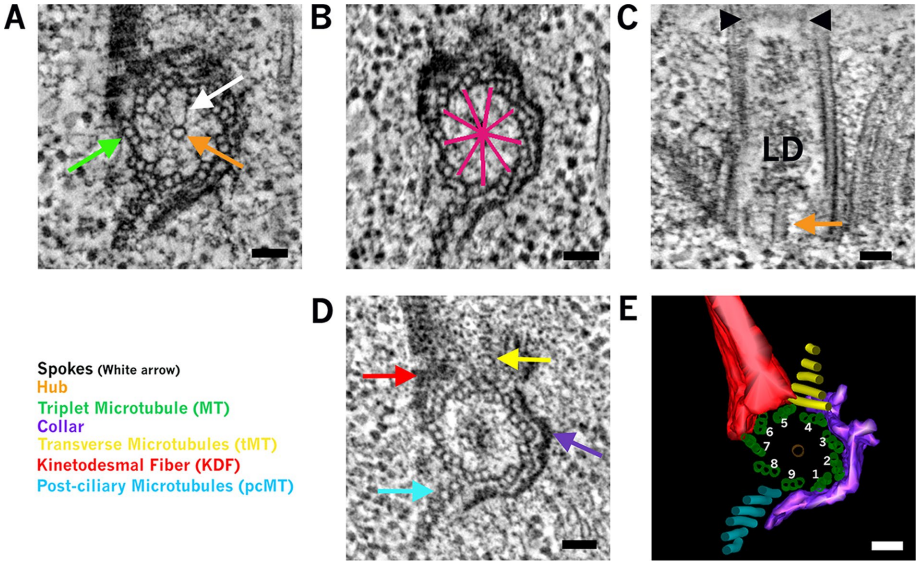

FIGURE 1: Electron tomography of *Tetrahymena* basal bodies. Images are oriented such that the top is directed toward the cell's anterior. Color representations of modeled structures are consistent with each other. (A) Cross-sectional view of the basal body. The cartwheel is at the basal body proximal end and is composed of a hub and nine spokes, which extend to the A-tubules of the basal body wall. (B) Basal body triplet microtubules are spaced at ~40° increments around the basal body cylinder, highlighted by magenta lines. (C) Longitudinal section of the basal body. The basal body luminal density (LD) is present between the top of the hub and the transition zone (arrowheads). (D) Accessory structures are asymmetrically associated with basal bodies. (E) Specific triplet microtubules, identified by number, are associated with accessory structures. Basal body triplet microtubules, green; kinetodesmal fiber, red; transverse microtubules, yellow; collar, purple; postciliary microtubules, light blue; hub, orange. Scale bars, 50 nm. See Supplemental Video S1.

The cartwheel structure resides at the basal body base or proximal end and comprises a central hub with nine spokes radiating outward and attaching to the A-tubule of each triplet microtubule. In centrioles, the cartwheel is transient and only present in assembling centrioles (Alvey, 1986; Strnad and Gönczy, 2008). Ultimately, centrioles and basal bodies have a highly conserved core structure with nine rotationally symmetric subunits that organize centrosomes and cilia, respectively. In the case of multiciliary arrays in both ciliates and vertebrate cells, these symmetrically organized basal bodies provide docking sites for asymmetrically localized appendage or accessory structures that anchor and position basal bodies (Allen, 1969; O'Toole and Dutcher, 2014; Pearson, 2014). This ensures a polarized ciliary beat pattern that is important for effective hydrodynamic flow.

In addition to the well-defined structural architecture of centrioles and basal bodies established by electron microscopy (Dippell, 1968; Allen, 1969; O'Toole *et al.*, 2003; Guichard *et al.*, 2012, 2013; Winey and O'Toole, 2014), genomic and proteomic studies identified many centriole and basal body protein components (Andersen *et al.*, 2003; Keller *et al.*, 2005; Kilburn *et al.*, 2007; Müller *et al.*, 2010). However, where and how these protein components function to build and maintain centrioles and basal bodies remain poorly defined.

The proteome of centriole 1 (Poc1) protein is a highly conserved and abundant centriole and basal body protein (Keller *et al.*, 2005, 2009; Kilburn *et al.*, 2007; Pearson *et al.*, 2009; Venoux *et al.*, 2013). Mutations in human Poc1 cause ciliopathies such as dwarfism, facial dysmorphology, insulin resistance, and rod-cone dystrophy (Sarig *et al.*, 2012; Shaheen *et al.*, 2012; Roosing *et al.*, 2014; Chen *et al.*, 2015; Geister *et al.*, 2015; Koparir *et al.*, 2015). Moreover, Poc1 loss disrupts normal primary ciliogenesis (Pearson *et al.*, 2009). Loss of Poc1 in the ciliate *Tetrahymena* and human cells causes basal body and centriole instability (Pearson *et al.*, 2009; Venoux *et al.*, 2013). Poc1 is a microtubule-binding protein and affects centriole length in human cells (Hames *et al.*, 2008; Keller *et al.*, 2009). Basal body triplet microtubules in *Tetrahymena* cells lacking Poc1 are disrupted (Pearson *et al.*, 2009). However, the mechanism by which Poc1 stabilizes triplet microtubules is not established.

In this study, we use cryofixation by high-pressure freezing/freeze substitution in combination with electron tomography to identify the three-dimensional architecture of *Tetrahymena* wild-type and poc1Δ basal bodies and their associated accessory structures. We reveal structural defects that are difficult or impossible to detect using conventional thin-section transmission electron microscopy and identify a role for Poc1 at the A-C linkers in coupling neighboring triplet microtubules of the basal body cylinder. Poc1 is important for maintaining A-C linker integrity, and cells lacking Poc1 display disrupted basal body structure and organization of the triplet microtubules. We propose that Poc1 ensures normal linkages between triplets and that when this connection is defective, the stability of basal bodies is compromised.

RESULTS

Symmetrically constructed basal bodies are associated with asymmetrically placed accessory structures

Ninefold symmetry in *Tetrahymena* basal bodies is established around the cartwheel (Figure 1A). The angle between the basal body center and each adjacent A-tubule occurs at ~40° increments around the basal body cylinder (Figure 1B). Distal to the cartwheel is a luminal density that extends from the top of the cartwheel to the terminal plate or transition zone, the site of axoneme formation (Figure 1C). As found by prior studies, the *Tetrahymena* basal body itself is symmetrically organized and continuous with the cilium (Marshall, 2012; O'Toole and Dutcher, 2014; Pearson, 2014; Bayless *et al.*, 2016).

In contrast to the symmetric organization of the core basal body structure, accessory structures provide asymmetric organization and regular spacing of basal bodies to establish directed ciliary beating and associated hydrodynamic flow (Wloga and Frankel, 2012; Galati *et al.*, 2014; Pearson, 2014). In multiciliated cells, basal bodies are positioned relative to each other and oriented relative to the global polarity of the cell (Beisson and Sonneborn, 1965; Tamm *et al.*, 1975; Zhang and Mitchell, 2016). Basal bodies of the ciliate *Tetrahymena* are organized in rows along the cell's anterior–posterior axis such that the anterior or posterior sides of the basal bodies refer to their geometry relative to the cellular polarity. Each ciliary row is made up of repeating units consisting of a basal body with its associated accessory structures (Figure 1, D and E, and Supplemental Video S1; Allen, 1969; Frankel and Jenkins, 1979; Jerka-Dziadosz *et al.*, 1995). The nonuniform positioning of accessory structures allows each triplet microtubule to be defined (Figures 1E and 2B; Lynn, 1981; Beisson and Jerka-Dziadosz, 1999; Wloga and Frankel, 2012). Triplet microtubules 1–4 are associated

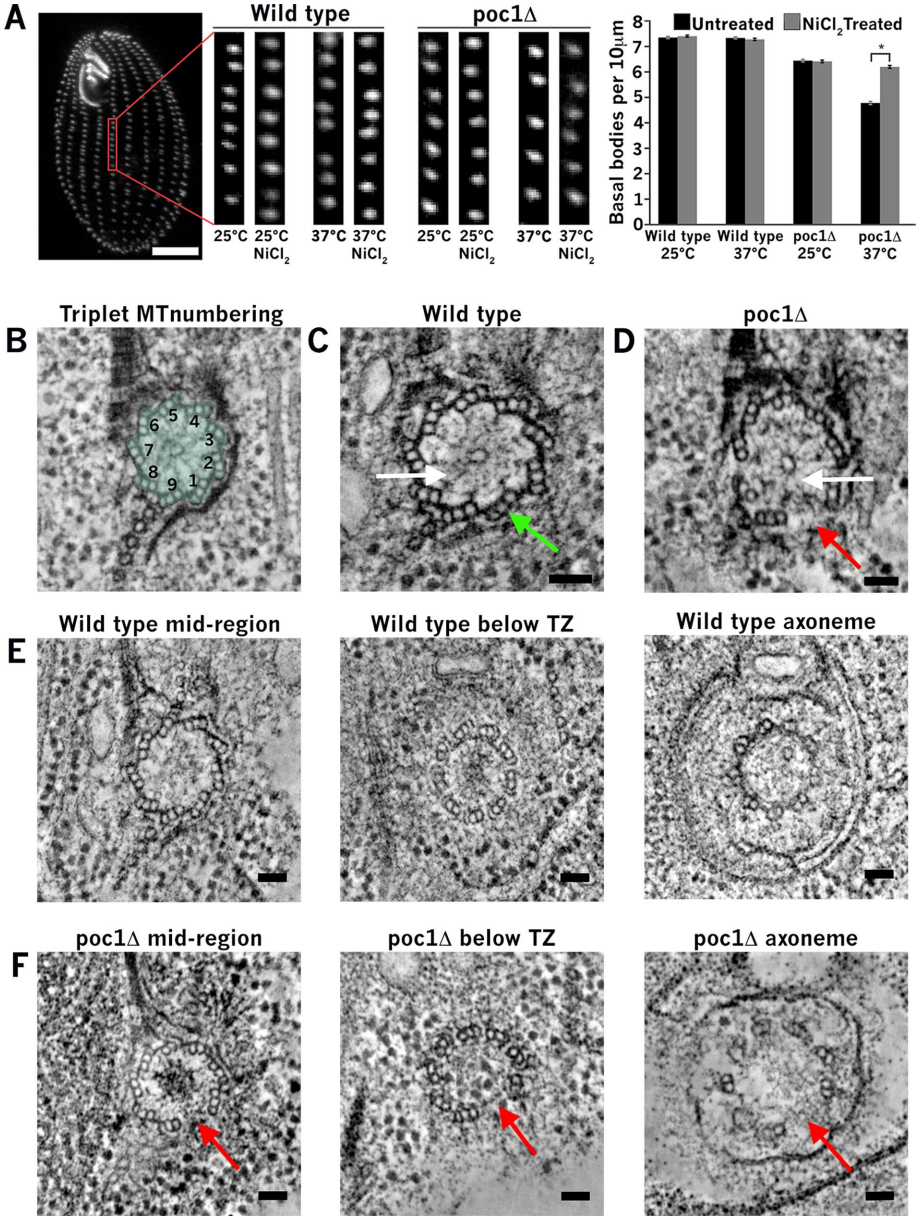

FIGURE 2: Triplet microtubules are absent in poc1Δ basal bodies. (A) Basal body disassembly in poc1Δ cells is rescued by inhibiting ciliary beating. Left, immunofluorescence image of a wild-type *Tetrahymena* cell showing the region where basal body number counts were taken. Scale bar, 10 μm. Middle, representative 10-μm insets of basal body rows used for determining basal body number in wild-type and poc1Δ cells. Right, quantification of basal body number per 10 μm in wild-type and poc1Δ cells. *$p < 0.001$; 300 basal body counts. (B) Triplet microtubules are identified with numbers as indicated. (C) Wild-type basal bodies have nine triplet microtubules (green arrow) with attached spokes (white arrow). (D) Comparable view of a poc1Δ basal body missing a triplet microtubule at position 1 (red arrow). A spoke (white arrow) radiates out toward the gap that is normally occupied by a triplet microtubule. (E, F) Series of tomographic slices through a wild-type basal body (E), and a poc1Δ basal body (F) missing a triplet at position 1 (red arrows) resulting in missing ciliary doublet microtubules. Images are taken at mid basal body (left), just below the transition zone (middle), and at the base of the ciliary axoneme (right). Scale bars, 50 nm.

with a densely stained structure at the proximal end of the basal body called the collar, which wraps around about one-third of the basal body circumference and extends distally to approximately one-third of the basal body length (Figure 1, D and E; Kilburn *et al.*, 2007). Despite the collar's distinctive morphology, its function and molecular composition are not known. On the anterior side of the basal body, associated with triplet microtubules 4 and 5, are the transverse microtubules (Figure 1, D and E). Also on the anterior side of the basal body, a striated fiber known in *Tetrahymena* as the kinetodesmal fiber is positioned at triplet microtubules 5–7 and extends both anteriorly and upward toward the plasma membrane (Figure 1, D and E). Finally, the postciliary microtubules are associated with triplet microtubules 8 and 9 and are oriented toward the posterior end of the cell (Figure 1, D and E). The *Tetrahymena* basal body is a symmetric cilium-organizing center whose asymmetric accessory structures position it within the polarized geometry of the cell.

Poc1 ensures the retention of basal body triplet microtubules

Basal bodies anchor cilia, and it is proposed that they withstand forces generated by ciliary beating (Lindemann and Kanous, 1997; Lindemann and Lesich, 2010; Vernon and Woolley, 2004; Riedel-Kruse *et al.*, 2007). We predict that the basal body structure described earlier is essential for basal bodies to resist these mechanical forces. To test this, we examined a *Tetrahymena* basal body mutant that causes basal body instability, poc1Δ. We previously found that poc1Δ cells exhibit an increased loss of basal bodies due to their disassembly over time (Pearson *et al.*, 2009). Basal bodies in poc1Δ cells normally disassemble upon temperature shift from 25 to 37°C (Figure 2A). In contrast, when ciliary beating and cell swimming are inhibited by treating cells with $NiCl_2$, we find that the basal body loss in poc1Δ cells is rescued. These results suggest that basal body disassembly in poc1Δ cells requires ciliary beating and that ciliary beating imposes forces on basal bodies that are resisted by Poc1 function.

As a microtubule-binding protein (Hames *et al.*, 2008), one hypothesis is that Poc1 stabilizes basal body triplet microtubules. Consistent with our prediction, triplet microtubule loss is observed in poc1Δ basal bodies, occurring in five of 18 basal bodies for which we have tomograms (28%; Figure 2D, red arrow; comparable wild type, Figure 2C; Supplemental Figure S1). No triplet microtubule loss is observed in wild-type cells. Triplet microtubule loss is complete through the basal body and extends as doublet loss into the cilium (Figure 2F, red arrows; comparable wild type, Figure 2E). Basal bodies were most often missing one whole triplet microtubule, although basal bodies missing as many as six triplet microtubules were observed (Supplemental Figure S1). The increased frequency of triplet microtubule loss may represent the progressive disassembly and eventual loss of basal bodies, as previously reported (Pearson *et al.*, 2009).

Of interest, specific triplet microtubules are preferentially lost in poc1Δ basal bodies. Combining tomographic and thin-section data of basal bodies missing triplet microtubules, we see that nine of 11 (82%) basal bodies are missing triplet microtubules at position 1 or 2 (Figure 2, D and F, and Supplemental Figure S1). These triplet microtubules are oriented toward the cell's posterior. The triplet microtubules that most commonly persist in poc1Δ basal bodies are those associated with the kinetodesmal fiber (Figures 1E and 2B, triplet microtubules 5–7), suggesting that a stabilizing interaction exists between these triplet microtubules and the kinetodesmal fiber. The kinetodesmal fiber, postciliary microtubules, transverse microtubules, and collar are all maintained in poc1Δ cells. Mutations in other genes that are known to affect basal body structure result in the loss of A- or C-tubules or possibly B- and C-tubules within triplet microtubules (Goodenough and StClair, 1975; Dutcher and Trabuco, 1998; Garreau de Loubresse *et al.*, 2001; Bayless *et al.*, 2012; Ross *et al.*, 2013). However, basal bodies in poc1Δ cells lose entire triplet microtubules, suggesting that Poc1 is required to organize and/or stabilize triplet microtubules. Moreover, posteriorly facing triplet microtubules are preferentially lost.

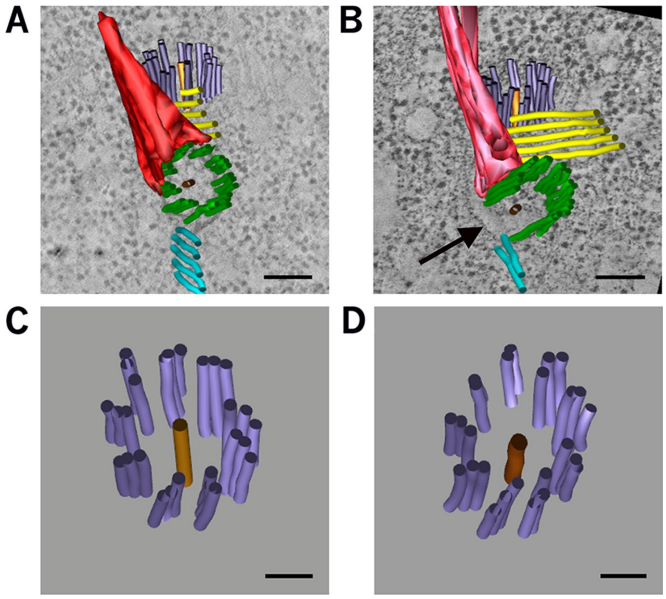

FIGURE 3: New poc1Δ basal bodies assemble with nine triplet microtubules. (A) Wild-type basal body duplication; new basal body length, 102 nm. Scale bar, 100 nm. See Supplemental Video S2. (B) The poc1Δ daughter basal body is normal despite the mother basal body missing two triplet microtubules (8 and 9; black arrow). The new basal body contains nine triplet microtubules (new basal body length, 105 nm). Scale bar, 100 nm. See Supplemental Video S3. (C, D) Model views of (C) the new wild-type basal body in A and (D) the new poc1Δ basal body in B. Two microtubules of the new poc1Δ basal body are out of the volume. New basal body triplet microtubules, lavender. Scale bars, 50 nm.

poc1Δ basal bodies assemble with ninefold symmetry

The observation that mature poc1Δ basal bodies are missing triplet microtubules led us to inquire into whether new basal bodies assemble with a complete set of nine triplet microtubules. Basal bodies in poc1Δ cells initiate new basal body assembly (Pearson *et al.*, 2009), and our results confirm that poc1Δ basal bodies are indeed competent to direct new basal body assembly (Figure 3 and Supplemental Videos S2 and S3). Of 18 basal bodies in the tomographic data set, 11 were assembling new basal bodies (Supplemental Figures S1 and S2 and Supplemental Videos S6 and S7). Each newly formed basal body contains a full complement of nine triplet microtubules, suggesting that Poc1 is not required to form new basal bodies with nine triplet microtubules but instead is required to stabilize them after their biogenesis (Figure 3D).

Basal bodies are formed orthogonally to existing basal bodies in what is called a "templated" assembly process. SAS-6, a major component of the cartwheel, is proposed to use the mother centriole as a template for the ninefold symmetry of the structure, which it then passes on to the daughter through translocation from mother to daughter (Fong *et al.*, 2014). This suggests that the architecture and ninefold symmetry of the mother centriole may be imposed on the daughter's structural formation. To further address this hypothesis, we asked whether poc1Δ basal bodies that are missing triplet microtubules are competent to generate new basal bodies. Of the duplicating basal body pairs, three contain mature basal bodies missing one or two triplet microtubules (Supplemental Figure S1). In all cases, new basal bodies assembling adjacent to defective basal bodies contain nine triplet microtubules. Although not definitive, these results suggest that the number of newly formed basal body triplet microtubules is not templated directly from the mother basal body's triplet microtubules (Figure 3B and Supplemental Video S3).

Basal body ninefold symmetry is established early in assembly by the cartwheel at the basal body's proximal end (Beisson and Wright, 2003). Poc1 localizes along the triplet microtubules of the basal body and is enriched proximally where the cartwheel attaches to the triplet microtubules (Keller *et al.*, 2009; Pearson *et al.*, 2009). We asked whether the asymmetric loss of triplet microtubules in poc1Δ cells is due to cartwheel disruption. The hub and spokes of the cartwheel are intact in poc1Δ basal bodies, even when basal bodies are missing one or more triplet microtubules (Figure 2D, white arrow; wild-type comparison, Figure 2C, white arrow). The 40° spacing between the remaining triplet microtubules is retained, with the exception of the gaps created by the missing triplet microtubules (Figure 2, D and F, red arrow). The ninefold symmetric organization of basal bodies is preserved in poc1Δ cells even when a triplet microtubule is lost. Thus Poc1 is not required to establish or maintain ninefold symmetry but instead to maintain structural elements of the basal body within the existing architecture. In addition, Poc1 and triplet microtubules are not required to maintain the cartwheel spokes.

Poc1 is required to organize the proximal ends of basal body triplet microtubules

To understand how Poc1 stabilizes the triplet microtubules of mature basal bodies, we next focused on the organization of basal body triplet microtubules. Even though the cartwheel and ninefold symmetry are unaffected in poc1Δ mutants, we observed subtle defects at the proximal ends of the basal bodies where the minus ends of microtubules are located. The proximal ends of wild-type basal bodies display a consistent alignment between neighboring triplet microtubule minus ends (Figure 4A; colored spheres mark microtubule ends). In contrast, poc1Δ triplet microtubule minus ends are not well aligned (Figure 4B; colored spheres mark microtubule ends). Variation in microtubule minus-end placement is evident in tomographic cross sections and includes variation both within and between triplet microtubules (Figure 4, D, red arrows and green arrow, and C, comparable wild type). We quantified this observation by measuring the microtubule minus-end distribution relative to an arbitrary plane in wild-type and poc1Δ basal bodies. The wild-type basal bodies show a tight distribution of distance from the plane, whereas poc1Δ basal bodies have a wider distribution of distance

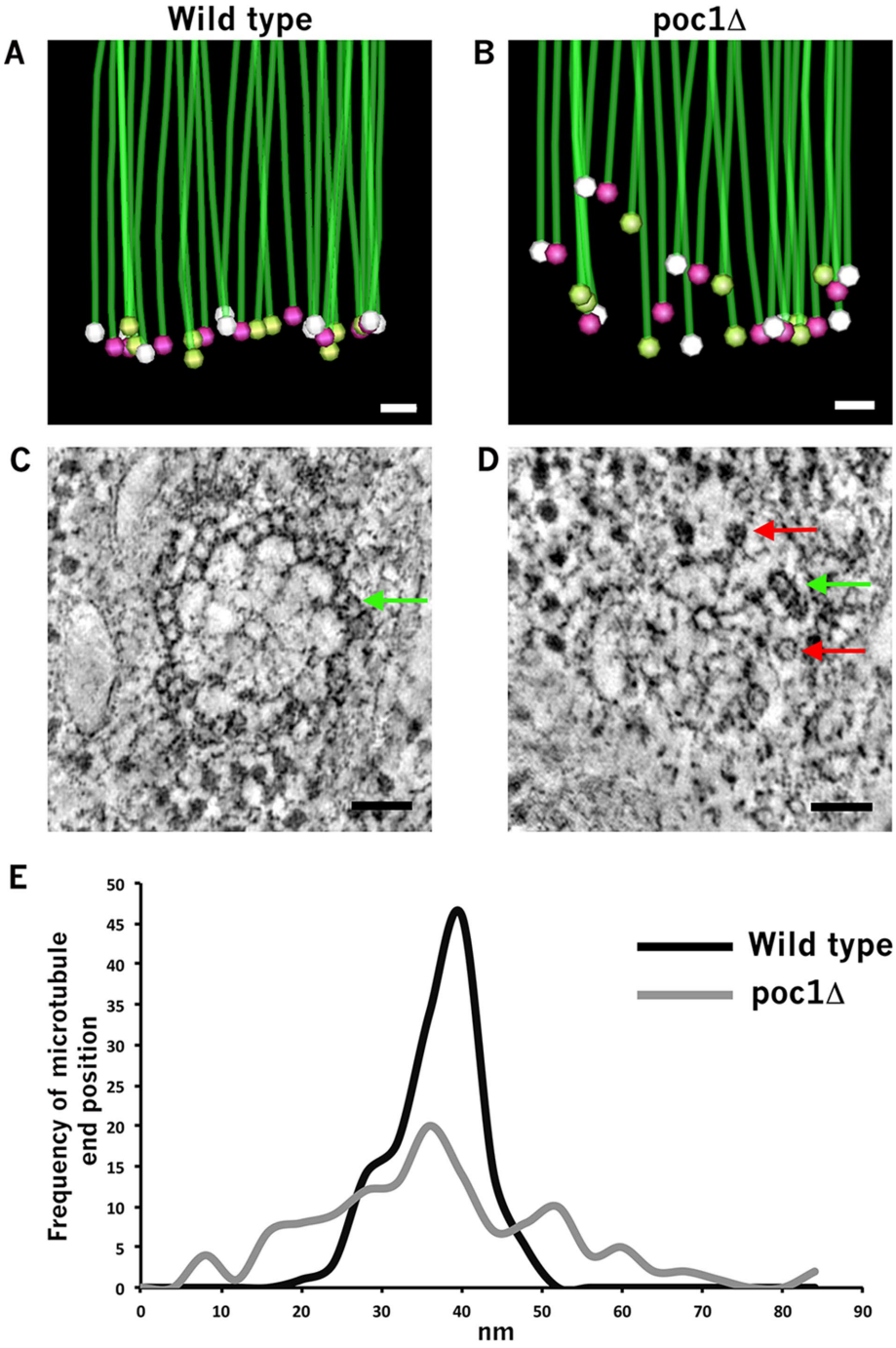

FIGURE 4: Proximal ends of triplet microtubules are disorganized in poc1Δ basal bodies. (A, B) Triplet microtubules are aligned at the proximal end of the basal body in wild-type cells (A) but are misaligned in poc1Δ basal bodies (B). Triplet microtubules, green; microtubule minus ends, light green (A-tubule), magenta (B-tubule), and white (C-tubule) spheres. Scale bars, 20 nm. (C) Wild-type microtubules originate in a similar plane, both individually and within triplet units (green arrow). (D) The poc1Δ triplet microtubules (red arrows highlight those triplets displaying only a visible A-tubule) and also whole triplet units (green arrow) are staggered at the basal body proximal end. (E) Frequency distribution of microtubule minus ends, demonstrating a tight distribution of wild-type microtubule minus ends (black) distinct from the broad distribution of poc1Δ microtubule minus ends (gray), $p < 0.001$. Five basal bodies each for wild type (135 microtubule ends) and poc1Δ (129 microtubule ends). Scale bars, 50 nm.

from the plane (Figure 4E). Of importance, Poc1 loss has no effect on basal body length, suggesting that, although the total basal body length is preserved, the overall arrangement of triplet microtubule minus ends is affected in poc1Δ basal bodies (poc1Δ basal body length, 400 ± 52 nm; wild-type basal body length, 388 ± 46 nm). Wild-type triplet microtubules at positions 1–4 tend to be slightly above the plane defined by the other triplet microtubules, possibly due to the inherent helical twist of the basal body, and this is enhanced in poc1Δ basal bodies. The shorter triplet microtubules observed at the basal body posterior face in wild-type cells suggests that there are asymmetries inherent in triplet microtubule populations. Moreover, this is accentuated in poc1Δ basal bodies. Of interest, these same triplet microtubules are commonly missing in poc1Δ basal bodies, suggesting that the displacement of triplet microtubules 1–4 at the proximal end of basal bodies in poc1Δ cells may contribute to the preferential loss of these triplet microtubules.

The poc1Δ-associated disruption of triplet microtubule organization might arise from defects in either microtubule nucleation or stability of existing microtubule minus ends. γ-Tubulin complexes stabilize microtubule minus ends, giving a capped appearance, whereas open or splayed structures indicate unstable minus ends (O'Toole *et al.*, 1999; Wiese and Zheng, 2000). O'Toole *et al.* (2003) reported that *Chlamydomonas* basal bodies have capped triplet microtubule ends, leading us to ask whether the triplet microtubule minus ends of poc1Δ basal bodies are also capped. Indeed, the microtubule minus ends of the A-, B-, and C-tubules of triplet microtubules in both wild-type and poc1Δ basal bodies are capped (Supplemental Figure S3), suggesting that the microtubule minus ends are stable and that the positioning of triplet microtubule ends is directed by additional structural constraints.

Poc1 is required for the helical organization of triplet microtubules

Basal body triplet microtubules are organized with a centripetal rotation along the length of the basal body (Anderson, 1972; Albrecht-Buehler, 1990; Paintrand *et al.*, 1992; Li *et al.*, 2012). The rotation of each triplet creates an iris diaphragm effect by which the triplet microtubules at the distal end of the basal body are more tangential to the basal body cylinder than are those at the proximal end (Albrecht-Buehler, 1990). This organization reveals coordinated linkage between the triplets and perhaps influences the positioning of triplet microtubule minus ends. Each triplet twists gradually over the length of the basal body, which is referred to as the twist angle (Figure 5A; Anderson, 1972; Li *et al.*, 2012). We tested whether the twist angle is affected

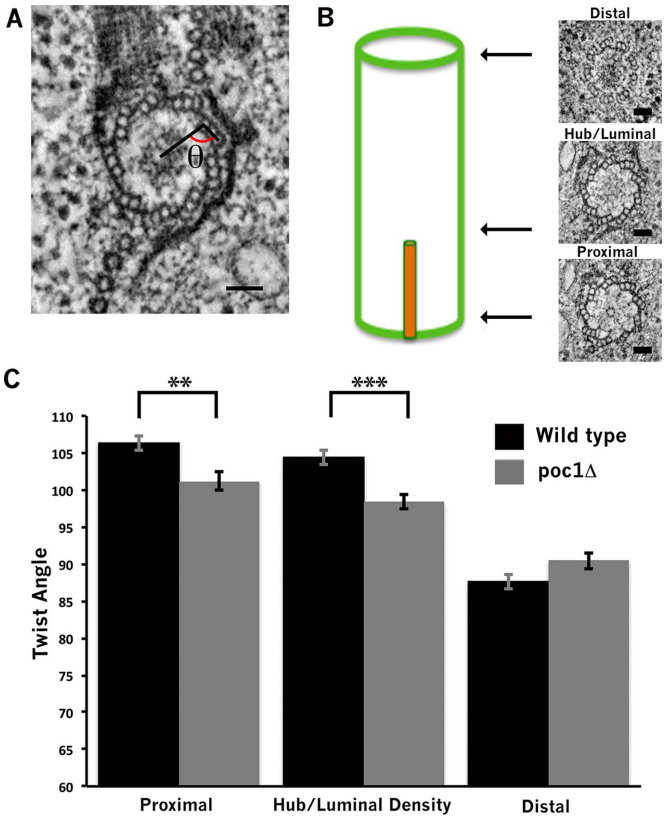

FIGURE 5: Poc1 loss disrupts the twist angle of triplet microtubule blades along the length of the basal body. (A) The twist angle is measured at the intersection of a line from the basal body center to the A-tubule and a line that bisects the triplet microtubules (black lines). The red arc denotes the measured angle (θ). (B) Schematic view of the basal body, with arrows indicating the positions of measurements and corresponding tomographic views. (C) Twist angle measurements for wild-type (black) and poc1Δ (gray) basal bodies. The mean with SE bars is displayed; $^{**}p < 0.005$, $^{***}p < 0.001$. Wild-type data set: proximal, 90 angles (10 basal bodies); hub/luminal density interface, 90 angles (10 basal bodies); distal, 45 angles (five basal bodies). The poc1Δ data set: proximal, 58 angles (seven basal bodies); hub/luminal density, 87 angles (10 basal bodies); distal, 69 angles (eight basal bodies). Scale bars, 50 nm.

by Poc1 loss at three defined positions along the basal body: the proximal end, the interface between the hub and luminal density, and the distal end (Figure 5B). We observed a decrease in twist angle from the proximal to the distal end in both wild-type and poc1Δ basal bodies (Figure 5C), consistent with previous studies (Anderson, 1972; Albrecht-Buehler, 1990; Li *et al.*, 2012). However, poc1Δ basal bodies have a significantly decreased triplet twist angle at the proximal end compared with wild-type basal bodies (wild type, 106 ± 1°; poc1Δ, 101 ± 1°; $p < 0.005$; Figure 5C). Similarly, the twist angle at the hub/luminal density interface is more diminished in poc1Δ basal bodies than in wild type (wild type, 104 ± 1°; poc1Δ, 98 ± 1°; $p < 0.001$; Figure 5C). At the distal end, there is no significant difference in twist angle between wild-type and poc1Δ (wild type, 88 ± 1°; poc1Δ, 90 ± 1°; Figure 5C). The poc1Δ basal bodies exhibit a shallower change in twist angle over the length of the basal body (from 101 to 90°) compared with wild type (from 106 to 88°). These results suggest that Poc1 is required to maintain proper triplet microtubule twist angle, most notably at the proximal end of basal bodies, where Poc1 preferentially localizes.

Poc1 promotes connections between triplet microtubules

The longitudinal twist angle of triplet microtubules is proposed to be influenced by intertriplet linkers, known as A-C linkers (Anderson, 1972; Albrecht-Buehler, 1990; Li *et al.*, 2012). A-C linkers connect triplet microtubules by bridging the outer edge of the A-tubule of one triplet microtubule to the inner edge of the C-tubule of the neighboring triplet (Figure 6A, middle). A-C linkers are at the proximal end of basal bodies, extending approximately one-third of the longitudinal basal body length (Figure 6A, left). The constituents of A-C linkers are unknown (Anderson, 1972; Albrecht-Buehler, 1990; Li *et al.*, 2012). We asked whether the decreased twist angle at the proximal end of poc1Δ basal bodies could arise from defects in A-C linkers. We first determined the cross-sectional width of the A-C linkers by measuring the distance from the A-tubule along the linker to the C-tubule of the adjoining triplet microtubule at the proximal end of basal bodies (Figure 6A, middle). The poc1Δ A-C linkers are shorter than wild-type A-C linkers (wild type, 12.3 ± 0.3 nm SD; poc1Δ, 11.4 ± 0.3 nm SD; $p < 0.05$; Figure 6A, right). Furthermore, A-C linkers are present only if neighboring triplet microtubules are intact, as A-C linkers are absent when triplet microtubules are positioned next to a missing triplet microtubule. This suggests that the A-C linker is either unable to form or is unstable without attachment to both the A- and the C-tubules. In summary, poc1Δ A-C linkers are shorter, coinciding with reduced twist angle, and A-C linkers require adjacent triplet microtubules for their presence.

Because A-C linkers are proposed to maintain the triplet microtubule angle along the length of the basal body, we next asked whether Poc1 is required for the spatial distribution or positioning of A-C linkers along the length of basal bodies. We began by analyzing the proximal distribution of A-C linkers. To quantify the proximal position of each A-C linker relative to the base of the basal body, we measured the distance from the minus end of the A-tubule to the first emergence of the A-C linker attached to that A-tubule (Figure 6B). Wild-type A-C linkers are uniformly distributed near A-tubule minus ends, whereas they are unevenly distributed and further from the A-tubule minus ends in the poc1Δ strain (Figure 6B; wild type, 11.6 ± 4.1 nm SD; poc1Δ, 33.7 ± 18.6 nm SD; $p < 0.001$). Thus Poc1 is required for the proximal positioning of A-C linkers within basal bodies.

Because the proximal distribution of A-C linkers is disrupted in poc1Δ basal bodies, we next asked whether the longitudinal length of the A-C linkers was altered (Figure 6C and Supplemental Videos S4 and S5). The A-C linker length was measured along the longitudinal axis of the basal body from the first visible connection at the basal body proximal end to the last visible connection at the distal end (Figure 6C). A-C linkers in wild-type basal bodies are of uniform length (151.8 ± 18.4 nm SD; Figure 6C). In contrast, the poc1Δ A-C linker longitudinal lengths are shorter and more variable (92.8 ± 26.3 nm SD; $p < 0.001$; Figure 6C). We could not observe a correlation between specific A-C linker length variability and triplet microtubule loss because the presence of the A-C linker appears to require the microtubule triplets. Nonetheless, it is clear that A-C linker width, position, and length are aberrant in poc1Δ basal bodies.

DISCUSSION

Poc1 is a conserved component of basal bodies and centrioles (Hodges *et al.*, 2010). The human genome has two paralogues of Poc1, and mutations in these genes give rise to a class of genetic diseases known as ciliopathies (Sarig *et al.*, 2012; Shaheen *et al.*, 2012; Roosing *et al.*, 2014; Chen *et al.*, 2015; Geister *et al.*, 2015; Koparir *et al.*, 2015). Poc1 plays a role in both ciliogenesis and centriole stability (Pearson *et al.*, 2009; Venoux *et al.*, 2013). This study

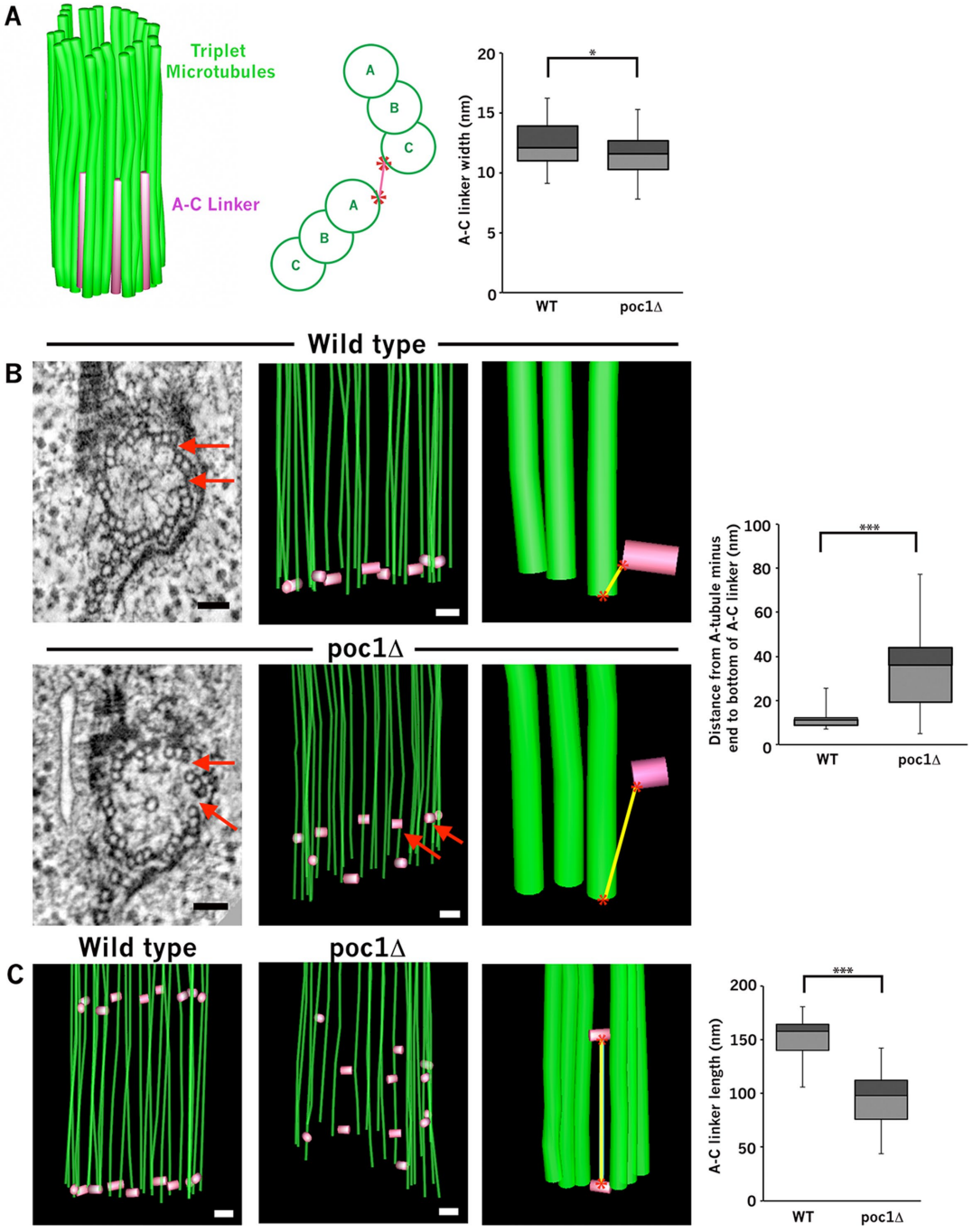

FIGURE 6: Poc1 is required for connections between triplet microtubules. (A) Left, diagram of a basal body with triplet microtubules and A-C linkers. Middle, schematic of A-C linker placement relative to the A-tubule from one triplet and the C-tubule of its neighbor. Red asterisks indicate the width measurement graphed on the right. Right, box-and-whisker plot showing the median, first and third quartile, minimum, and maximum measurements of A-C linker width. *$p < 0.05$; wild type, $N = 54$; poc1Δ, $N = 49$. (B) Wild-type A-C linker proximal position vs. poc1Δ A-C linker proximal position. Left, tomographic cross sections at basal body proximal ends. Red arrows highlight A-C linkers (in wild type) or lack of A-C linkers (in poc1Δ). Middle, positions of the A-C linker proximal ends are depicted as pink bars. Bottom middle, red arrows correspond to red arrows on the left, demonstrating that the proximal ends of these A-C linkers emerge more distally than others in the same basal body. Yellow line from the A-tubule minus end to the emergence of the A-C linker demonstrates how the measurements included in the box-and-whisker plot on the far right were made. Far right, box-and-whisker plot of the median, first and third quartile, minimum, and maximum measurements of A-C linker proximal placement in wild-type and poc1Δ basal bodies. ***$p < 0.001$; wild type, $N = 21$; poc1Δ. $N = 22$. (C) Models of basal bodies in longitudinal view showing the A-C linker boundaries in pink. Left, wild type; second, poc1Δ; third, schematic illustrating how the A-C linker span is measured (yellow line); far right, box-and-whisker plot of the median, first and third quartile, minimum, and maximum measurements of A-C linker length in wild-type and poc1Δ basal bodies. ***$p < 0.001$; wild-type, $N = 45$; poc1Δ, $N = 40$. Triplet microtubules, green; A-C linker boundaries, pink. Scale bars, 50 nm (B, left), 20 nm (B, middle, C). See Supplemental Videos S4 and S5.

used electron tomography to determine the structural defects that lead to basal body loss. Previously unrecognized defects in triplet microtubule organization were identified at the proximal ends of basal bodies in *Tetrahymena* cells lacking Poc1. We propose that Poc1 has an important role in maintaining A-C linkers between triplet microtubules, and failure of these linkers in poc1Δ cells leads to the disorganization and loss of triplet microtubules and ultimately the disassembly of basal bodies.

We argue that the structural defects observed in poc1Δ basal bodies can be explained by the loss of normal A-C linker function. These include disorganized proximal or minus ends of the triplet microtubules, decrease of triplet microtubule twist angles, and complete loss of triplet microtubules. Indeed, there is evidence that A-C linkers influence the twist angle of triplet microtubules (Anderson, 1972; Li *et al.*, 2012). This model suggests a molecular interaction between Poc1, the triplet microtubules, and the component(s) of the A-C linker. Alternatively, Poc1 may function as a component of the A-C linker. Poc1 contains a sevenfold WD-40 repeated domain that is essential for its function (Pearson *et al.*, 2009). It is possible that the interaction between Poc1 and the A-C linkers occurs via the WD-40 domain. In addition, Poc1 localizes at basal body proximal ends and along the microtubule cylinder walls (Pearson *et al.*, 2009) and demonstrates an association with microtubules (Hames *et al.*, 2008; Keller *et al.*, 2009). These data suggest that Poc1 may interact with both microtubules and A-C linkers to stabilize basal bodies in the face of forces exerted from ciliary beating.

The cartwheel resides at the proximal end of the basal body and is important for establishing ninefold symmetry early in centriolar and basal body assembly. Mutants encoding components of the cartwheel are unable to maintain correct triplet spacing in their basal bodies. Instead of preserving ninefold symmetry, basal bodies in several of these mutants form open and/or closed cylinders with abnormal triplet microtubule numbers (Hiraki *et al.*, 2007; Nakazawa *et al.*, 2007; Jerka-Dziadosz *et al.*, 2010; Bayless *et al.*, 2012). The poc1Δ basal bodies, on the other hand, maintain ninefold symmetry and a normal cartwheel with regular 40° spacing of the A-tubules around the hub of the cartwheel, even when triplet microtubules are missing.

Of interest, *Tetrahymena* poc1Δ basal bodies lacking a full complement of nine triplet microtubules are capable of supporting assembly of new basal bodies that contain nine triplet microtubules. This demonstrates that formation of triplet microtubules in new basal bodies may not be dependent on an intact existing basal body. However, our finding does not rule out the model proposed by Fong *et al.* (2014) in which a major constituent of the cartwheel, SAS-6, acquires ninefold symmetry from the existing mother basal body, which it then transposes to the developing daughter. Moreover, we do not know when the triplet microtubules of the mother basal body are lost relative to initiation of new daughter basal body assembly. The daughter basal bodies are short and closely positioned relative to their mothers, suggesting that these newly formed basal bodies may have assembled when the mother basal body was already missing triplet microtubules (Supplemental Figure S1). Of importance, these studies show that poc1Δ basal bodies are initially assembled as complete structures and subsequently lose triplet microtubules. It remains to be discovered at what stage of assembly and maturation poc1Δ basal bodies begin to disassemble. Because basal body disassembly in poc1Δ cells requires normal ciliary beating, we suggest that forces from ciliary beating promote basal body disassembly, as was found with loss of the Bld10 basal body component (Figure 2A; Bayless *et al.*, 2012).

A-C linkers are present between the triplet microtubules at the proximal one-third of the basal body, and their placement and length are defective in poc1Δ cells. Combined with the observation that the absence of Poc1 leads to the loss of complete triplet microtubules, Poc1 in all likelihood stabilizes basal bodies by organizing or stabilizing the A-C linkers. We observed that triplet microtubule loss is most frequent at positions oriented toward the posterior of the cell. Computational models predict that triplet microtubules near the posterior face of basal bodies experience compressive forces from ciliary beating and therefore may be vulnerable to disassembly if the basal body is compromised (Lindemann and Kanous, 1997; Vernon and Woolley, 2004; Riedel-Kruse *et al.*, 2007). Factors such as force distribution and proximity to accessory structures may contribute to the biased triplet microtubule loss in poc1Δ basal bodies. Our results also demonstrate that lack of triplet microtubules results in the absence of corresponding doublet microtubules in the cilium, demonstrating that Poc1 is required for building functional cilia. This may account for the slower-swimming phenotype previously described in poc1Δ *Tetrahymena* cells (Pearson *et al.*, 2009). Finally, loss of individual triplet microtubules may cause a progressive loss of additional triplet microtubules as forces increase on the remaining triplet microtubules, suggesting that A-C linkers are important for both triplet microtubule and ultimately basal body stability.

In spite of the nearly global presence of A-C linkers in centrioles and basal bodies containing triplet microtubules, little is known about their composition and function. Our results reveal defects in basal body organization and stability when A-C linker position is disrupted in poc1Δ cells. How basal body twist angle affects basal body stability, force resistance, and ciliogenesis are interesting avenues for future research. In addition, further studies are needed to determine a mechanistic relationship between Poc1 and A-C linkers.

MATERIALS AND METHODS

Cell culture and growth conditions

The poc1 knockout was generated in the *Tetrahymena thermophila* cell line B2086. The poc1Δ mutation is lethal at high temperatures, requiring cells be grown at a semipermissive temperature of 30°C. Wild-type B2086 cells were used as a control. To optimize basal body duplication events for electron microscope imaging, cells were grown in nutrient-rich medium to mid log phase (super proteose peptone [SPP]; 2% protease peptone, 0.2% glucose, 0.1% yeast extract, and 0.003% Fe-EDTA; Orias *et al.*, 2000), shifted to starvation medium overnight (10 mM Tris, pH 7.4), and then resuspended in 2% SPP for 90 min to 2.5 h.

Preparation of cells for electron microscopy

Cells were gently spun out of SPP, resuspended in a cryoprotectant of 15% dextran (molecular weight 9000–11,000; Sigma-Aldrich, St. Louis, MO) and 5% bovine serum albumin in 2% SPP, and gently spun to concentrate the cells. A small volume was transferred to a sample holder and high-pressure frozen using a Wohlwend Compact 02 high-pressure freezer (Technotrade International, Manchester, NH). After low-temperature freeze substitution in 0.25% glutaraldehyde and 0.1% uranyl acetate in acetone, cells were slowly infiltrated with Lowicryl HM20 resin and polymerized. For routine electron microscopy, serial thin sections (80 nm) were cut and stained for 5 min with aqueous uranyl acetate and 3 min with Reynold's lead stain. A Philips CM100 electron microscope was used to image sections. For electron tomography, sections of 300–350 nm

were cut and poststained for 8 min with aqueous uranyl acetate and 5 min with Reynold's lead citrate. Colloidal gold (15 nm) was applied to each side of the grid as fiducial markers for tilt series image alignment.

Measuring basal body frequency

Basal body frequency was quantified as previously described (Bayless *et al.*, 2012). Quantification of basal body frequency was performed by counting the number of basal bodies of a 10-μm region along a ciliary row in the medial region of the cell. Ciliary rows around the entire circumference of the cell were quantified. All experiments used five measurements per cell over 20 cells. All experiments were repeated in triplicate for a total of 300 counts. All counts were corrected for cell length by multiplying the number of basal bodies by the ratio of wild-type to mutant cell length. For ciliary beating inhibition experiments, cells were arrested for 24 h before treatment with 200 μM $NiCl_2$. Cells were maintained in the arrest for an additional 24 h, after which the basal body frequency was quantified. Ciliary inhibition by treatment of cells with $NiCl_2$ was confirmed by visualizing decreased cellular swimming.

Electron tomography and analysis

Dual-axis tilt series (−60 to +60°) of selected basal bodies were collected on an FEI Tecnai F30 IVEM (FEI, Eindhoven, Netherlands). Tomograms of both wild-type cells and poc1Δ cells were generated using the IMOD software package, which allows the user to view and display tomographic reconstructions at high resolution and in any orientation (Kremer *et al.*, 1996; Mastronarde, 1997; O'Toole *et al.*, 2007). Three-dimensional models were created using the IMOD software package. In total, 24 tomograms were collected from 20 wild-type cells (25 basal bodies) and 14 tomograms from 12 poc1Δ cells (18 basal bodies).

Analysis and measurements

Microtubule triplet twist angle. Screenshots were taken in the slicer window in IMOD and opened with ImageJ (National Institutes of Health, Bethesda, MD). The angle of each triplet microtubule was determined with the angle tool in ImageJ.

MT end analysis. Programs were run in IMOD (resamplemod, imodextract, and model2point) to orient microtubule walls in the *y*-axis for all data sets used in this analysis. A plane was set in the *x*-axis at an arbitrary distance from the base of the basal body. Variance in microtubule end position was acquired and binned based on frequency distribution. Chi-squared tests were performed to determine statistical significance. Values were normalized and graphed.

A-C linker parameters. A-C linker width was measured in IMOD by drawing a contour spanning the width of the A-C linker between the A-tubule of one triplet microtubule and the C-tubule of the neighboring triplet. Measurements were taken at the proximal end of the basal body where the A-C linker emerges. A-C linker distance from the base of the basal body was acquired in IMOD by drawing a contour from the minus end of the A-tubule to the most proximal part of the A-C linker attached to that A-tubule. A-C linker length was determined in IMOD by drawing a contour from the most proximal visible presence of the A-C linker to the most distal visible presence of the A-C linker. All of the data were analyzed using box-and-whisker plots. Two-tailed Student's *t* tests were performed to determine *p* values.

ACKNOWLEDGMENTS

We thank Alex Stemm-Wolf for helpful discussions and critical reading of the manuscript, David Mastronarde for assistance with IMOD data analysis, and Eileen O'Toole for help and useful suggestions with IMOD. C.G.P. is funded by National Institutes of Health/National Institute of General Medical Sciences Grant GM099820, the Pew Biomedical Scholars Program, and the Boettcher Foundation. M.W. is supported by National Institutes of Health/National Institute of General Medical Sciences Grant GM074746.

REFERENCES

Abal M, Keryer G, Bornens M (2005). Centrioles resist forces applied on centrosomes during G2/M transition. Biol Cell 97, 425–434.

Albrecht-Buehler G (1990). The iris diaphragm model of centriole and basal body formation. Cell Motil Cytoskeleton 17, 197–213.

Allen RD (1969). The morphogenesis of basal bodies and accessory structures of the cortex of the ciliated protozoan Tetrahymena pyriformis. J Cell Biol 40, 716–733.

Alvey PL (1986). Do adult centrioles contain cartwheels and lie at right angles to each other? Cell Biol Int Rep 10, 589–598.

Andersen JS, Wilkinson CJ, Mayor T, Mortensen P, Nigg EA, Mann M (2003). Proteomic characterization of the human centrosome by protein correlation profiling. Nature 426, 570–574.

Anderson RG (1972). The three-dimensional structure of the basal body from the rhesus monkey oviduct. J Cell Biol 54, 246–265.

Bayless BA, Galati DF, Pearson CG (2016). Tetrahymena basal bodies. Cilia 5, 1.

Bayless BA, Giddings TH, Winey M, Pearson CG (2012). Bld10/Cep135 stabilizes basal bodies to resist cilia-generated forces. Mol Biol Cell 23, 4820–4832.

Beisson J, Jerka-Dziadosz M (1999). Polarities of the centriolar structure: morphogenetic consequences. Biol Cell 91, 367–378.

Beisson J, Sonneborn TM (1965). Cytoplasmic inheritance of the organization of the cell cortex in paramecium aurelia. Proc Natl Acad Sci USA 53, 275–282.

Beisson J, Wright M (2003). Basal body/centriole assembly and continuity. Curr Opin Cell Biol 15, 96–104.

Chen J-H, Segni M, Payne F, Huang-Doran I, Sleigh A, Adams C, Consortium UK10K, Savage DB, O'Rahilly S, Semple RK, *et al.* (2015). Truncation of POC1A associated with short stature and extreme insulin resistance. J Mol Endocrinol 55, 147–158.

Dippell RV (1968). The development of basal bodies in paramecium. Proc Natl Acad Sci USA 61, 461–468.

Dutcher SK, Trabuco EC (1998). The UNI3 gene is required for assembly of basal bodies of Chlamydomonas and encodes delta-tubulin, a new member of the tubulin superfamily. Mol Biol Cell 9, 1293–1308.

Fliegauf M, Benzing T, Omran H (2007). When cilia go bad: cilia defects and ciliopathies. Nat Rev Mol Cell Biol 8, 880–893.

Fong CS, Kim M, Yang TT, Liao J-C, Tsou M-FB (2014). SAS-6 assembly templated by the lumen of cartwheel-less centrioles precedes centriole duplication. Dev Cell 30, 238–245.

Frankel J, Jenkins LM (1979). A mutant of Tetrahymena thermophila with a partial mirror-image duplication of cell surface pattern. II. Nature of genic control. J Embryol Exp Morphol 49, 203–227.

Galati DF, Bonney S, Kronenberg Z, Clarissa C, Yandell M, Elde NC, Jerka-Dziadosz M, Giddings TH, Frankel J, Pearson CG (2014). DisAp-dependent striated fiber elongation is required to organize ciliary arrays. J Cell Biol 207, 705–715.

Garreau de Loubresse N, Ruiz F, Beisson J, Klotz C (2001). Role of delta-tubulin and the C-tubule in assembly of Paramecium basal bodies. BMC Cell Biol 2, 4.

Geister KA, Brinkmeier ML, Cheung LY, Wendt J, Oatley MJ, Burgess DL, Kozloff KM, Cavalcoli JD, Oatley JM, Camper SA (2015). LINE-1 mediated insertion into Poc1a (protein of centriole 1 A) causes growth insufficiency and male infertility in mice. PLoS Genet 11, e1005569.

Gibbons IR, Grimstone AV (1960). On flagellar structure in certain flagellates. J Biophys Biochem Cytol 7, 697–716.

Gönczy P (2015). Centrosomes and cancer: revisiting a long-standing relationship. Nat Rev Cancer 15, 639–652.

Goodenough UW, StClair HS (1975). BALD-2: a mutation affecting the formation of doublet and triplet sets of microtubules in Chlamydomonas reinhardtii. J Cell Biol 66, 480–491.

Guichard P, Hachet V, Majubu N, Neves A, Demurtas D, Olieric N, Fluckiger I, Yamada A, Kihara K, Nishida Y, *et al.* (2013). Native architecture of the centriole proximal region reveals features underlying its 9-fold radial symmetry. Curr Biol 23, 1620–1628.
Guichard P, Desfosses A, Maheshwari A, Hachet V, Dietrich C, Brune A, Ishikawa T, Sachse C, Gönczy P (2012). Cartwheel architecture of Trichonympha basal body. Science 337, 553.
Hames RS, Hames R, Prosser SL, Euteneuer U, Lopes CAM, Moore W, Woodland HR, Fry AM (2008). Pix1 and Pix2 are novel WD40 microtubule-associated proteins that colocalize with mitochondria in Xenopus germ plasm and centrosomes in human cells. Exp Cell Res 314, 574–589.
Hiraki M, Nakazawa Y, Kamiya R, Hirono M (2007). Bld10p constitutes the cartwheel-spoke tip and stabilizes the 9-fold symmetry of the centriole. Curr Biol 17, 1778–1783.
Hodges ME, Scheumann N, Wickstead B, Langdale JA, Gull K (2010). Reconstructing the evolutionary history of the centriole from protein components. J Cell Sci 123, 1407–1413.
Jerka-Dziadosz M, Gogendeau D, Klotz C, Cohen J, Beisson J, Koll F (2010). Basal body duplication in Paramecium: the key role of Bld10 in assembly and stability of the cartwheel. Cytoskeleton (Hoboken) 67, 161–171.
Jerka-Dziadosz M, Jenkins LM, Nelsen EM, Williams NE, Jaeckel-Williams R, Frankel J (1995). Cellular polarity in ciliates: persistence of global polarity in a disorganized mutant of Tetrahymena thermophila that disrupts cytoskeletal organization. Dev Biol 169, 644–661.
Keller LC, Geimer S, Romijn E, Yates J, Zamora I, Marshall WF (2009). Molecular architecture of the centriole proteome: the conserved WD40 domain protein POC1 is required for centriole duplication and length control. Mol Biol Cell 20, 1150–1166.
Keller LC, Romijn EP, Zamora I, Yates JR III, Marshall WF (2005). Proteomic analysis of isolated Chlamydomonas centrioles reveals orthologs of ciliary-disease genes. Curr Biol 15, 1090–1098.
Kilburn CL, Pearson CG, Romijn EP, Meehl JB, Giddings TH, Culver BP, Yates JR, Winey M (2007). New Tetrahymena basal body protein components identify basal body domain structure. J Cell Biol 178, 905–912.
Koparir A, Karatas OF, Yuceturk B, Yuksel B, Bayrak AO, Gerdan OF, Sagiroglu MS, Gezdirici A, Kirimtay K, Selcuk E, *et al.* (2015). Novel POC1A mutation in primordial dwarfism reveals new insights for centriole biogenesis. Hum Mol Genet 24, 5378–5387.
Kremer JR, Mastronarde DN, McIntosh JR (1996). Computer visualization of three-dimensional image data using IMOD. J Struct Biol 116, 71–76.
Li S, Fernandez J-J, Marshall WF, Agard DA (2012). Three-dimensional structure of basal body triplet revealed by electron cryo-tomography. EMBO J 31, 552–562.
Lindemann CB, Kanous KS (1997). A model for flagellar motility. Int Rev Cytol 173, 1–72.
Lindemann CB, Lesich KA (2010). Flagellar and ciliary beating: the proven and the possible. J Cell Sci 123, 519–528.
Lynn DH (1981). The organization and evolution of microtubular organelles in ciliated protozoa. Biol Rev 56, 243–292.
Marshall WF (2012). Centriole asymmetry determines algal cell geometry. Curr Opin Plant Biol 15, 632–637.
Mastronarde DN (1997). Dual-axis tomography: an approach with alignment methods that preserve resolution. J Struct Biol 120, 343–352.
Müller H, Schmidt D, Steinbrink S, Mirgorodskaya E, Lehmann V, Habermann K, Dreher F, Gustavsson N, Kessler T, Lehrach H, *et al.* (2010). Proteomic and functional analysis of the mitotic Drosophila centrosome. EMBO J 29, 3344–3357.
Nakazawa Y, Hiraki M, Kamiya R, Hirono M (2007). SAS-6 is a cartwheel protein that establishes the 9-fold symmetry of the centriole. Curr Biol 17, 2169–2174.
Nigg EA, Raff JW (2009). Centrioles, centrosomes, and cilia in health and disease. Cell 139, 663–678.
Orias E, Hamilton EP, Orias JD (2000). Tetrahymena as a laboratory organism: useful strains, cell culture, and cell line maintenance. Methods Cell Biol 62, 189–211.
O'Toole ET, Dutcher SK (2014). Site-specific basal body duplication in Chlamydomonas. Cytoskeleton (Hoboken) 71, 108–118.
O'Toole ET, Giddings TH, Dutcher SK (2007). Understanding microtubule organizing centers by comparing mutant and wild-type structures with electron tomography. Methods Cell Biol 79, 125–143.
O'Toole ET, Giddings TH, McIntosh JR, Dutcher SK (2003). Three-dimensional organization of basal bodies from wild-type and δ-tubulin deletion strains of Chlamydomonas reinhardtii. Mol Biol Cell 14, 2999–3012.
O'Toole ET, Winey M, McIntosh JR (1999). High-voltage electron tomography of spindle pole bodies and early mitotic spindles in the yeast Saccharomyces cerevisiae. Mol Biol Cell 10, 2017–2031.
Paintrand M, Moudjou M, Delacroix H, Bornens M (1992). Centrosome organization and centriole architecture: their sensitivity to divalent cations. J Struct Biol 108, 107–128.
Pearson CG (2014). Choosing sides–asymmetric centriole and basal body assembly. J Cell Sci 127, 2803–2810.
Pearson CG, Osborn DPS, Giddings TH, Beales PL, Winey M (2009). Basal body stability and ciliogenesis requires the conserved component Poc1. J Cell Biol 187, 905–920.
Riedel-Kruse IH, Hilfinger A, Howard J, Jülicher F (2007). How molecular motors shape the flagellar beat. HFSP J 1, 192–208.
Roosing S, Lamers IJC, de Vrieze E, van den Born LI, Lambertus S, Arts HH, POC1B Study Group, Peters TA, Hoyng CB, Kremer H, *et al.* (2014). Disruption of the basal body protein POC1B results in autosomal-recessive cone-rod dystrophy. Am J Hum Genet 95, 131–142.
Ross I, Clarissa C, Giddings TH, Winey M (2013). ε-Tubulin is essential in Tetrahymena thermophila for the assembly and stability of basal bodies. J Cell Sci 126, 3441–3451.
Sarig O, Nahum S, Rapaport D, Ishida-Yamamoto A, Fuchs-Telem D, Qiaoli L, Cohen-Katsenelson K, Spiegel R, Nousbeck J, Israeli S, *et al.* (2012). Short stature, onychodysplasia, facial dysmorphism, and hypotrichosis syndrome is caused by a POC1A mutation. Am J Hum Genet 91, 337–342.
Shaheen R, Faqeih E, Shamseldin HE, Noche RR, Sunker A, Alshammari MJ, Al-Sheddi T, Adly N, Al-Dosari MS, Megason SG, *et al.* (2012). POC1A truncation mutation causes a ciliopathy in humans characterized by primordial dwarfism. Am J Hum Genet 91, 330–336.
Strnad P, Gönczy P (2008). Mechanisms of procentriole formation. Trends Cell Biol 18, 389–396.
Tamm SL, Sonneborn TM, Dippell RV (1975). The role of cortical orientation in the control of the direction of ciliary beat in Paramecium. J Cell Biol 64, 98–112.
Venoux M, Tait X, Hames RS, Straatman KR, Woodland HR, Fry AM (2013). Poc1A and Poc1B act together in human cells to ensure centriole integrity. J Cell Sci 126, 163–175.
Vernon GG, Woolley DM (2004). Basal sliding and the mechanics of oscillation in a mammalian sperm flagellum. Biophys J 87, 3934–3944.
Waters AM, Beales PL (2011). Ciliopathies: an expanding disease spectrum. Pediatr Nephrol 26, 1039–1056.
Wiese C, Zheng Y (2000). A new function for the γ-tubulin ring complex as a microtubule minus-end cap. Nat Cell Biol 2, 358–364.
Winey M, O'Toole E (2014). Centriole structure. Philos Trans R Soc Lond B Biol Sci 369, 20130457.
Wloga D, Frankel J (2012). From molecules to morphology: cellular organization of Tetrahymena thermophila. Methods Cell Biol 109, 83–140.
Zhang S, Mitchell BJ (2016). Basal bodies in Xenopus. Cilia 5, 2.